Generalization of Surface Junction Modeling for Composite Objects in an SIE/MoM Formulation Using a Systematic Approach

Joon Shin, Allen W. Glisson, and Ahmed A. Kishk
Department of Electrical Engineering
The University of Mississippi
University, MS 38677

Abstract— **This paper discusses the modeling of various kinds of surface junctions in an SIE/MoM formulation applied to complex objects consisting of arbitrarily shaped conducting and dielectric bodies. Methods of describing various types of junctions and systematically incorporating them in numerical solutions are presented. The procedures are of interest for the speci c application of arbitrarily shaped dielectric resonator antennas and their associated feed structures and packaging. An E-PMCHWT formulation in conjunction with a moment method procedure using multi-domain RWG basis functions is presented to deal with such general junctions. Some results are veri ed with the FDTD method.**

Index Terms— **surface junction modeling, composite object, SIE/MoM, E-PMCHWT, dielectric resonator antenna, multi-domain basis function, FDTD**

I. INTRODUCTION

THE modeling of general surface junctions in an SIE/MoM (Surface Integral Equation / Method of Moments) formulation is considered in this work. The speci c application leading to this study is that of Dielectric Resonator (DR) antennas. Since an experimental study of a cylindrical DR antenna was reported in 1983 [1], this antenna has drawn continued interest because of its small size, ef cienc y, and potential ability to perform multiple antenna tasks via simple mode coupling mechanisms. The con guration of a DR antenna may range from a very simple one that allows analytic solutions to a very complex one. A typical structure for a DR antenna is a DR element of high dielectric constant excited by a single feed such as a microstripline or coaxial cable. Various shapes and combinations of DR elements as well as various feed structures have been suggested, however, which may improve the antenna performance in the areas of bandwidth, power handling, and antenna ef cienc y. Rigorous SIE analysis methods for non-trivial DR antenna con gurations have been available mainly for Body of Revolution (BoR) objects [2,3]. DR antennas have also been treated with the constraint of a multi-layered environment [4,5]. where the dielectric layers are assumed to be of in nite extent. In this work we consider the modeling of general junctions encountered in such arbitrary con gurations of DR antennas, which may include general 3D (Three-Dimensional) composite objects, using an SIE/MoM method with RWG (Rao-Wilton-Glisson) basis functions. Arbitrary con gurations here refer to an arbitrary number of dielectric regions, arbitrary compositions of conductors and dielectrics, general excitations, etc., as well as arbitrary shapes.

The dif culty with an arbitrary 3D composite object comes mainly from the modeling of surface junctions. To model a surface junction, it has been considered necessary to properly enforce the electromagnetic boundary conditions and the continuity of the currents at the junction. For a given junction this may be accomplished easily, and the associated unknown currents and basis functions are assigned accordingly. However, for an arbitrary con guration consisting of different types of junctions, neither the formulation nor the implementation is trivial. A usual approach might be to implement the junction models only for some limited number of cases and to make modi cations when need arises for a speci c type of junction. A similar argument is true in general, but to a somewhat lesser extent, for the MoM technique regarding the number of dielectric regions and the geometry con guration. The objective of this study is to develop a rigorous yet ef cient numerical method for EM (Electromagnetic) modeling of arbitrary composite structures, which allows one, as a particular application, to ef ciently try various con gurations of DR antennas to optimize the performance.

The junction modeling problem has been considered in previous works for conducting surfaces [6], for dielectric surfaces [7], simple combinations of BoR objects [2,3,8,9], and general conducting, dielectric, resistive, and impedance boundary condition surfaces [10]. Finally, Kolundzija has also reported extensive junction modeling of composite objects [11]. A more detailed account for the junction modeling as well as various SIE/MoM formulations is found in his coauthored book [12]. Kolundzija employed a PMCHWT (Poggio-Miller-Chung-Harrington-Wu-Tsai) formulation [13-15] , which has been commonly been referred to as a PMCHW formulation, and entire domain basis functions de ned over bilinear surfaces, which required fewer unknowns, and thus electrically larger problem can be solved more ef ciently . The extent of his surface junction modeling is the same as ours. He describes the junction modeling in terms of *doublets*, while we do so using *multi-domain basis functions* and *multiplicity of basis function*. He treats an *open* metalic surface located at a dielectric interface as two *closed* metalic surfaces, while we treat it directly as another class of surfaces, which seems simpler to implement. While [11] presents general rules,

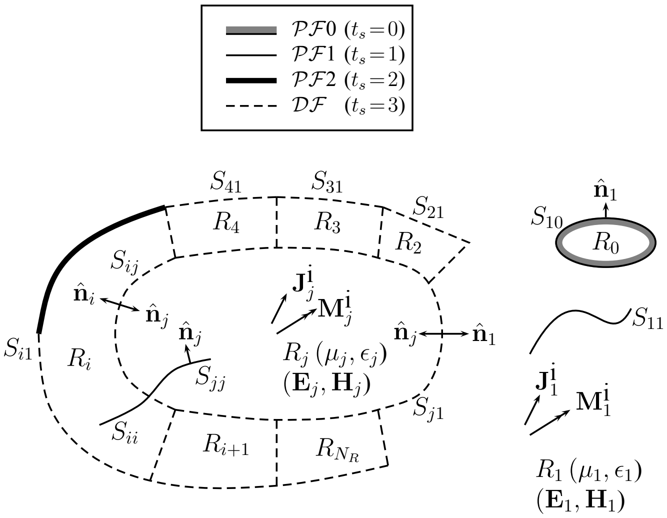

Fig. 1. General geometry under consideration.

we present speci c formulas for systematic and automatic construction of basis functions, and all kinds of junctions are classi ed into only a few cases, for which speci c formulas are given. In general we feel that our description of junction modeling is elegant and systematic. The advantage of such a systematic approach is that it enables a developer to set up a framework that can be easily extended to include new features more easily while maintaining code clarity. It should be noted that another procedure for junction treatment has also been recently described in [16].

II. FORMULATION

A. Problem Description

The geometry under consideration is a general inhomogeneous body with N_R dielectric regions, each of which may contain conducting bodies as well as impressed sources as shown in Fig. 1. The regions have permittivities ϵ_i and permeabilities μ_i, where $i = 1, \cdots, N_R$. Both ϵ_i and μ_i may be complex to represent lossy materials. Non-zero thickness conducting bodies denoted by R_0 may occupy any parts of the space. In nitely thin conducting bodies can reside in any region, at interfaces between regions, or they may penetrate from one region to another. All conductors are considered to be PEC (Perfect Electric Conductor) material. One of the regions, region R_1 in Fig. 1, may be of in nite extent. The total elds in each region are denoted by $\mathbf{E}_i$ and $\mathbf{H}_i$, where $i = 0, 1, 2, \cdots, N_R$, for electric and magnetic elds, respectively, and $i = 0$ denotes PEC regions with $\mathbf{E}_0 = \mathbf{H}_0 = \mathbf{0}$. The time variation, $e^{j\omega t}$, is assumed and suppressed throughout.

Any two adjacent regions, R_i and R_j, are separated by a surface denoted by $S_{ij}(t_s, t, f)$, where t_s is the type of the surface, and t and f are the 'to-region' and the 'from-region' of the surface, respectively, which de ne the region connectivity and the surface orientation. The interface between a non-zero thickness conducting body and a dielectric region also forms a surface denoted in the same way with the 'from-region' being region zero. An in nitely thin conducting body in a dielectric region forms yet another type of surface with the 'from-region' being the same as the 'to-region. Thus, there are four types of surfaces speci ed by t_s:

(i) $\mathcal{PF}0$ ($t_s = 0$) — Interface between a conducting body and a dielectric region,
(ii) $\mathcal{PF}1$ ($t_s = 1$) — In nitely thin conducting body within a dielectric region,
(iii) $\mathcal{PF}2$ ($t_s = 2$) — In nitely thin conducting body between two dielectric regions, and
(iv) $\mathcal{DF}(t_s = 3)$ — Dielectric interface between two dielectric regions.

These surface types are graphically represented by thick shaded, solid, thick solid, and dashed lines, respectively, in Fig. 1. We refer to $\mathcal{PF}0$, $\mathcal{PF}1$, and $\mathcal{PF}2$ collectively by $\mathcal{PF}$ (PEC faces).

When more than two surfaces meet at a curved line segment, they form a junction. Depending on the numbers and types of the surfaces at a junction, there are a variety of possible junction types, all of which are considered in this study.

Each region R_i is surrounded by a closed surface S_i^C and is associated with an inward normal unit vector $\hat{\mathbf{n}}_i$. The surface interface between regions R_i and R_j, if one exists, is denoted as S_{ij}, for any i and j, $i = 1, \cdots, N_R,\ j = 0, 1, \cdots, N_R$. Thus, S_i^C is the set of all interface surfaces S_{ij}, where j represents all region numbers that interface with region R_i. Note that $S_{ij} = S_{ji}$ for $j \neq 0$; however, the normal unit vectors $\hat{\mathbf{n}}_i$ and $\hat{\mathbf{n}}_j$ are in opposite directions to each other on S_{ij}.

B. The Field Equivalences

According to the equivalence principle [17], the original problem can be decomposed into N_R auxiliary problems, one for each dielectric region. To obtain the auxiliary problem for region R_i, the impressed sources of the original problem are retained only in region R_i and the boundaries of the region are replaced by equivalent surface currents radiating in a homogeneous medium with the constitutive parameters of region R_i. Electric currents are used for the conducting surfaces, while electric and magnetic currents are used for the dielectric boundaries. The electric and magnetic currents appearing on opposite sides of a dielectric interface in different auxiliary problems are taken equal in magnitude and opposite in direction to assure the continuity of the tangential eld components on these boundaries as they are continuous in the original problem. In this procedure, the elds produced within the region boundaries by the equivalent currents and the impressed sources in region R_i must be the same as those in the original problem, while the zero eld is chosen to exist outside these boundaries. The electric and magnetic currents along S_i^C are then $\mathbf{J}_i = \hat{\mathbf{n}}_i \times \mathbf{H}_i$ and $\mathbf{M}_i = \mathbf{E}_i \times \hat{\mathbf{n}}_i$, respectively.

A system of surface integro-differential equations can be obtained by enforcing the boundary conditions of continuity of the tangential components of electric eld on the conducting surfaces and both electric and magnetic elds on the dielectric surfaces. This results in the E-PMCHWT (Electric-PMCHWT) formulation [9] when there is no junction in the problem. For problems having general junctions, however, it is not easy to express the integral equation system explicitly apart from the testing procedure. Thus the system of integral equations is presented in the next section after describing the junction modeling and the basis functions.

C. Modeling of Junctions in the Moment Method Solution

Arbitrarily shaped surfaces are discretized in triangular patches and the equivalent surface currents are approximated by expansions in the RWG basis functions on the patches [18], which are expressed as

$$\mathbf{J}(\mathbf{r}) \cong \sum_{n=1}^{N_{T_j}} I_n \mathbf{B}_n^{T_j}(\mathbf{r}; S_{T_{n+}}, S_{T_{n-}}) \tag{1}$$

where

$$\mathbf{B}_n^{T_j}(\mathbf{r}) = \begin{cases} \pm \boldsymbol{\rho}_{n^\pm}/h_{n^\pm}, & \mathbf{r} \in S_{T_{n\pm}} \\ \mathbf{0}, & \text{otherwise}, \end{cases} \tag{2}$$

N_{T_j} is the number of electric basis functions, and $S_{T_{n\pm}}$ are the positive/negative domains or the from-/to- faces of the basis function, respectively. For magnetic currents, $\{\mathbf{B}_n^{T_m}\}_{n=1}^{N_{T_m}}$ can be de ned similarly. The testing functions $\mathbf{T}_n^{T_j}$ and $\mathbf{T}_n^{T_m}$ are also taken to be the same as (2). With the basis and testing functions de ned we have a matrix equation

$$\begin{bmatrix} \mathbf{Z}^{T_j\,T_j} & \mathbf{T}^{T_j\,T_m} \\ \mathbf{T}^{T_m\,T_j} & \mathbf{Y}^{T_m\,T_m} \end{bmatrix} \begin{bmatrix} |I^{T_j}\rangle \\ |I^{T_m}\rangle \end{bmatrix} = \begin{bmatrix} |V^{T_j}\rangle \\ |V^{T_m}\rangle \end{bmatrix}. \tag{3}$$

When there are general surface junctions, the current related to an unknown coef cient may exist on many different surfaces. In such cases, the expression (1) is not rigorous enough. For example, there is an electric current on a dielectric surface in the region R_i equivalent problem and another one o wing in the opposite direction in the region R_j problem, represented by '$-I_n$' as shown in Fig. 2(a). The expression in (1) for the electric currents has this sort of implication for the basis functions $\mathbf{B}_n^{T_j}$ when the domain of the unknown involves a dielectric interface, i.e., the single current coef cient I_n represents the current on both sides of the dielectric interface and one must identify which side of the interface carries the current coef cient with the negative sign.

When more than two dielectric surfaces meet at a junction, this scheme does not work. Thus for general junctions, we seek another way of expressing the generalized current more rigorously. We will use two different basis functions for the same unknown coef cient related to a dielectric surface as shown in Fig. 2(b). In other words, the unknown coef cient has a multiplicity of two when it represents the electric or magnetic current on the dielectric face. The current direction on each side of the interface in this case is accounted for by the direction of the basis function (Fig. 2(b)). This procedure is easily extended to account for a junction of multiple interfaces.

Extending this to the general case, the generalized current is de ned in terms of the generalized basis functions as

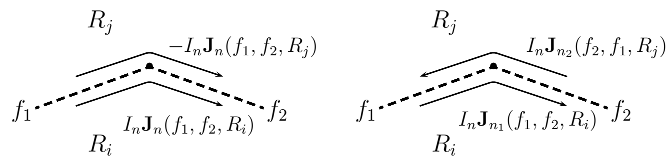

(a) Conventional representation (b) New representation

Fig. 2. Two methods of representing basis functions.

$$\mathbf{C}(\mathbf{r}) = \{\mathbf{J}(\mathbf{r}), \mathbf{M}(\mathbf{r})\} = \{\sum_{n=1}^{N_{T_j}} I_n \mathbf{B}_n(\mathbf{r}), \sum_{n=1+N_{T_j}}^{N} I_n \mathbf{B}_n(\mathbf{r})\} \tag{4}$$

where each $\mathbf{B}_n$ now represents τ_n simple basis functions as indicated below:

$$\mathbf{B}_n(\mathbf{r}) = \begin{cases} \mathbf{B}_k^{T_j}(\mathbf{r}), \text{ with } k = n, & n \le N_{T_j} \\ \mathbf{B}_k^{T_m}(\mathbf{r}), \text{ with } k = n - N_{T_j}, & n > N_{T_j} \end{cases} \tag{5}$$

where

$$\begin{aligned} N &= N_{T_j} + N_{T_m} \\ \mathbf{B}_k^{T_j}(\mathbf{r}) &= \sum_{v=1}^{\tau_k} \mathbf{B}_{k_v}^{T_j}(\mathbf{r}; ff_{k_v}, tf_{k_v}, R_{k_v}) \quad (6) \\ \mathbf{B}_k^{T_m}(\mathbf{r}) &= \sum_{v=1}^{\tau_k} \mathbf{B}_{k_v}^{T_m}(\mathbf{r}; ff_{k_v}, tf_{k_v}, R_{k_v}) \quad (7) \\ \mathbf{B}_{n_v} &= \text{the } v^{th} \text{ basis function of } I_n,\ v = 1, ..., \tau_n \\ \mathbf{B}_{k_v}^{T_j}, \mathbf{B}_{k_v}^{T_m} &= \text{RWG basis function de ned over the} \\ &\quad \text{corresponding patches as in (2)} \\ \tau_n &= \text{multiplicity of the unknown coef cient, } I_n \\ &= \begin{cases} n_{dfn}, & n_{dfn} = n_{tf} \\ n_{dfn} + 1, & \text{otherwise} \end{cases} \quad (8) \end{aligned}$$

$$\begin{aligned} n_{tf} &= \text{total number of faces connected} \\ n_{dfn} &= \text{number of dielectric faces related to } I_n \\ ff_{n_v}, tf_{n_v} &= \text{from-face and to-face of } \mathbf{B}_{n_v}. \\ R_{n_v} &= \text{region of } \mathbf{B}_{n_v}. \end{aligned}$$

Notice that there is one-to-one correspondence between $\mathbf{B}_{n_v}^{T_j}$ or $\mathbf{B}_{n_v}^{T_m}$ and the parameter set $\{ff_{n_v}, tf_{n_v}, R_{n_v}\}$. The numbers of unknowns and basis functions for a given junction or edge are determined from the types and numbers of the faces connected to the junction by considering proper boundary conditions at the junction. The methods of determining them and systematically incorporating them in the MoM solutions have been developed and presented in Appendix, where $\mathbf{J}_n$ and $\mathbf{M}_n$ are used instead of $\mathbf{B}_n^{T_j}$ and $\mathbf{B}_n^{T_m}$, respectively. The generalized testing functions $\{\mathbf{T}_m^{T_j}\}_{m=1}^{N_{T_j}}$, $\{\mathbf{T}_m^{T_m}\}_{m=1}^{N_{T_m}}$, and $\{\mathbf{T}_m\}_{m=1}^{N}$ are also de ned in a similar manner. We also de ne $\mathbf{C}_i$, the generalized current for the region R_i equivalent problem, as

$$\mathbf{C}_i(\mathbf{r}) = \{\mathbf{J}_i(\mathbf{r}), \mathbf{M}_i(\mathbf{r})\} \tag{9}$$

where

$$\mathbf{J}_i(\mathbf{r}) = \sum_{n=1}^{N_{T_j}} I_n \sum_{v=1}^{\tau_n} \delta^S_{n_v i} \mathbf{B}_{n_v}(\mathbf{r}; ff_{n_v}, tf_{n_v}, R_{n_v}) \tag{10}$$

$$\mathbf{M}_i(\mathbf{r}) = \sum_{n=N_{T_j}+1}^{N} I_n \sum_{v=1}^{\tau_n} \delta^S_{n_v i} \mathbf{B}_{n_v}(\mathbf{r}; ff_{n_v}, tf_{n_v}, R_{n_v}) \tag{11}$$

$$\begin{aligned} \delta^S_{n_v i} &= \text{source contribution coef cient} \\ &= \begin{cases} 1, & R_{n_v} = R_i \\ 0, & \text{otherwise} \end{cases}. \end{aligned}$$

With the set of basis functions in (4)–(7), one may apply the boundary conditions of tangential eld continuity at each subdomain of the basis functions. By merely applying the boundary conditions, however, the total number of equations may be greater than the number of the unknowns because of the multiplicity of some unknowns related to junctions. The usual methods of solving equations apply only when the number of equations equals to the number of unknowns, N. While the solution of an overdetermined system is certainly possible, it would increase the memory requirements to store the additional equations, and we prefer to generate equations that are equivalent to those we would obtain if modeling the junction in the usual manner.

Such a set of N equations can be obtained by taking the n^{th} integral equation as the set of simultaneous integral equations (or summation of them) which satisfy the proper boundary conditions on the subdomains of the basis functions ($\mathbf{B}_{n_v}, v = 1, ..., \tau_n$) related to the unknown coef cient, I_n. It is possible to obtain such a surface integral equation system by testing with the generalized testing functions as follows

$$\begin{aligned} &\sum_{i=1}^{N_R} \langle\, \mathbf{E}_i^{scat}(\mathbf{C}_i), \sum_{u=1}^{\tau_m} \delta^F_{r_{m_u} i}\, \mathbf{T}_{m_u} \,\rangle = \\ &\qquad -\sum_{i=1}^{N_R} \langle\, \mathbf{E}_i^{inc}, \sum_{u=1}^{\tau_m} \delta^F_{r_{m_u} i}\, \mathbf{T}_{m_u} \,\rangle, \\ &\qquad m = 1, 2, \ldots, N_{T_j} \end{aligned} \tag{12}$$

$$\begin{aligned} &\sum_{i=1}^{N_R} \langle\, \mathbf{H}_i^{scat}(\mathbf{C}_i), \sum_{u=1}^{\tau_m} \delta^F_{r_{m_u} i}\, \mathbf{T}_{m_u} \,\rangle = \\ &\qquad -\sum_{i=1}^{N_R} \langle\, \mathbf{H}_i^{inc}, \sum_{u=1}^{\tau_m} \delta^F_{r_{m_u} i}\, \mathbf{T}_{m_u} \,\rangle, \\ &\qquad m = N_{T_j}+1, \ldots, N_{T_j}+N_{T_m}, \end{aligned} \tag{13}$$

where

$$\begin{aligned} \langle\, \mathbf{f}, \mathbf{g} \,\rangle &= \int_S \mathbf{f} \cdot \mathbf{g}\, ds \\ r_{m_u} &= \text{region number of the testing function, } \mathbf{T}_{m_u}, \\ \delta^F_{r_{m_u} i} &= \text{ eld contribution coef cient} \\ &= \begin{cases} 1, & i = r_{m_u} \text{ (i.e., } R_i = R_{r_{m_u}}) \\ 0, & \text{otherwise} \end{cases} \end{aligned}$$

and ($\mathbf{E}_i^{scat}$, $\mathbf{H}_i^{scat}$) and ($\mathbf{E}_i^{inc}$, $\mathbf{H}_i^{inc}$) are the scattered elds due to $\mathbf{C}_i$ and incident elds, respectively. Equations (12) and (13) are the E-PMCHWT formulation [9] extended to general junctions.

The meaning of (12) is that the scattered and incident electric elds are tested by the electric testing functions. The testings are summed over the entire region ($i = 1, 2, \ldots, N_R$). However, the Kronecker delta function, $\delta^F_{r_{m_u} i}$, deselects the corresponding inner products if the region of the testing function, $\mathbf{T}_{m_u}$, is not R_i. The meaning of (13) is similar. The only difference is that the magnetic elds are tested with the magnetic testing functions as indicated by the range of the indices of the testing functions.

The electric and magnetic eld operators, E_i^J, E_i^M, H_i^J, and H_i^M, are de ned in terms of the magnetic vector, electric vector, electric scalar, and magnetic scalar potential functions $\mathbf{A}, \mathbf{F}, \Phi$, and Ψ, respectively, as [17]

$$\begin{aligned} \mathbf{E}_i(\mathbf{J}, \mathbf{M}) &= E_i^J \mathbf{J} + E_i^M \mathbf{M} \\ &= \{-j\omega \mathbf{A}_i - \nabla \Phi_i\} + \{-\frac{1}{\epsilon_i} \nabla \times \mathbf{F}_i\} \end{aligned} \tag{14}$$

$$\begin{aligned} \mathbf{H}_i(\mathbf{J}, \mathbf{M}) &= H_i^J \mathbf{J} + H_i^M \mathbf{M} \\ &= \{\frac{1}{\mu_i} \nabla \times \mathbf{A}_i\} + \{-j\omega \mathbf{F}_i - \nabla \Psi_i\}, \end{aligned} \tag{15}$$

where $\mathbf{E}_i$ and $\mathbf{H}_i$ are the electric and magnetic elds at the point $\mathbf{r} \in R_i$ due to the currents $\mathbf{J}$ and $\mathbf{M}$ on a speci ed surface, S_C. The surface S_C may be a subset of S_i^C, the closed surface of the region R_i, which supports equivalent currents, or it may be a source surface within the region R_i that supports impressed currents. However, there are situations in which no explicit impressed currents exist and the impressed elds are speci ed, for example, by incident plane wave. In (14) and (15), the subscript i represents the region number in which the elds or the potentials are evaluated. The potential functions are de ned as

$$\mathbf{A}_i(\mathbf{r}) = \mu_i \int_{S_C} \mathbf{J}(\mathbf{r}')\, G_i(\mathbf{r}, \mathbf{r}')\, ds' \tag{16}$$

$$\mathbf{F}_i(\mathbf{r}) = \epsilon_i \int_{S_C} \mathbf{M}(r')\, G_i(\mathbf{r}, \mathbf{r}')\, ds' \tag{17}$$

$$\Phi_i(\mathbf{r}) = \frac{1}{\epsilon_i} \int_{S_C} \sigma_e(\mathbf{r}')\, G_i(\mathbf{r}, \mathbf{r}')\, ds' \tag{18}$$

$$\Psi_i(\mathbf{r}) = \frac{1}{\mu_i} \int_{S_C} \sigma_m(\mathbf{r}')\, G_i(\mathbf{r}, \mathbf{r}')\, ds', \tag{19}$$

where the electric and magnetic surface charge densities σ_e and σ_m are related to the surface currents through the equations of continuity,

$$\sigma_e(\mathbf{r}) = -\frac{\nabla_S \cdot \mathbf{J}(\mathbf{r})}{j\omega} \tag{20}$$

$$\sigma_m(\mathbf{r}) = -\frac{\nabla_S \cdot \mathbf{M}(\mathbf{r})}{j\omega}. \tag{21}$$

In (16)–(19), $G_i(\mathbf{r}, \mathbf{r}')$ is the scalar homogeneous region Green's function and is de ned as

$$G_i(\mathbf{r}, \mathbf{r}') = \frac{e^{-jk_i R}}{4\pi R}, \tag{22}$$

where $R=|\mathbf{r}-\mathbf{r}'|$ is the distance between the eld point $\mathbf{r}\in R_i$ and the source point $\mathbf{r}'\in S_C$, and $k_i=\omega\sqrt{\mu_i\epsilon_i}$ is the wave number of the region R_i.

Substituting $\mathbf{C}_i$ of (4) into (12) and (13), the impedance matrix and excitation vector elements in (3), $Z_{mn}^{T_jT_j}$ and $V_m^{T_j}$, for example, are expressed as

$$\begin{aligned} Z_{mn}^{T_jT_j} &= \sum_{i=1}^{N_R} \langle\, \mathbf{E}_i^{scat}(\sum_{v=1}^{\tau_n}\delta^S_{r_{n_v}i}\mathbf{B}_{n_v}(\mathbf{r}')),\ \sum_{u=1}^{\tau_m}\delta^F_{r_{m_u}i}\mathbf{B}_{m_u}(\mathbf{r})\,\rangle \\ &= \sum_{i=1}^{N_R}\sum_{v=1}^{\tau_n}\sum_{u=1}^{\tau_m}\delta^S_{r_{n_v}i}\delta^F_{r_{m_u}i}\langle\, \mathbf{E}_i^{scat}(\mathbf{B}_{n_v}(\mathbf{r}')),\ \mathbf{B}_{m_u}(\mathbf{r})\,\rangle \\ &= \sum_{i=1}^{N_R}\sum_{v=1}^{\tau_n}\sum_{u=1}^{\tau_m}\delta^Z_{r_{m_u}r_{n_v}i}\langle\, E_i^J\mathbf{J}_{n_v}(\mathbf{r}'),\ \mathbf{J}_{m_u}(\mathbf{r})\,\rangle \\ &= \sum_{i=1}^{N_R}\sum_{v=1}^{\tau_n}\sum_{u=1}^{\tau_m}\delta^Z_{r_{m_u}r_{n_v}i}Z^{T_jT_j}_{m_un_v} \\ &\quad m=1,\ldots,N_{T_j}\ \text{ and }\ n=1,\ldots,N_{T_j} \end{aligned} \tag{23}$$

$$V_m^{T_j} = -\sum_{i=1}^{N_R}\sum_{u=1}^{\tau_m}\delta^F_{r_{m_u}i}\,\langle\,\mathbf{E}_i^{inc},\ \mathbf{J}_{m_u}(\mathbf{r})\rangle,\quad m=1,\ldots,N_{T_j}, \tag{24}$$

respectively, where

$$\begin{aligned} Z^{T_jT_j}_{m_un_v} &= \text{contribution from } \mathbf{J}_{n_v}(\mathbf{r}')/\mathbf{J}_{m_u}(\mathbf{r}) \text{ interaction} \\ &= \langle\, E_i^J\mathbf{J}_{n_v}(\mathbf{r}'),\ \mathbf{J}_{m_u}(\mathbf{r})\,\rangle \\ \delta^Z_{r_{m_u}r_{n_v}i} &= \text{Z contribution coef cient} \\ &= \delta^S_{r_{n_v}i}\delta^F_{r_{m_u}i} = \begin{cases} 1, & r_{m_u}=r_{n_v}=i \\ 0, & \text{otherwise,}\end{cases} \end{aligned} \tag{25}$$

$\mathbf{B}_{n_v}$ is denoted by $\mathbf{J}_{n_v}$ to signify the electric currents, and E_i^J is the electric eld operator de ned in (14). Notice that the generalized testing functions are the same as the basis functions.

The meaning of (23) is that $Z^{T_jT_j}_{m_un_v}$ is the interaction between $\mathbf{B}_n$ and $\mathbf{T}_m=\mathbf{B}_m$. The interaction is expressed by testing the scattered electric eld due to the source currents $\mathbf{B}_n$ with the testing functions $\mathbf{T}_m$. Since $\mathbf{B}_n$ and $\mathbf{T}_m$ are multi-domain basis and testing functions, the testings are summed over the entire region ($i=1,2,\ldots,N_R$). Examples of the expressions for the testing equations and resultant matrix elements are provided for speci c situations in Appendix B of [19].

It is worth noting that the triply indexed Kronecker delta functions select only terms whose related basis and testing functions have the same region as R_i, where i is the summation index. Although the expression for $Z_{mn}^{T_jT_m}$ in (23) contains the complicated-looking triple summation, typically only a few terms are left, e.g., only two terms for a dielectric surface, due to the Kronecker delta functions, and this notation automatically takes care of general multiple surface junctions.

The evaluation of the inner products of $\langle\, E_i^J\mathbf{J}_{n_v}(\mathbf{r}'),\ \mathbf{J}_{m_u}(\mathbf{r})\,\rangle$ and $\langle\,\mathbf{E}_i^{inc},\ \mathbf{J}_{m_u}(\mathbf{r})\,\rangle$ in (23) and (24), respectively, has been done using the approximate testing procedure explained in [18].

Other impedance matrix and excitation vector elements in (3) are obtained similarly from (12) and (13) as follows

$$\begin{aligned} T_{mn}^{T_jT_m} &= \sum_{i=1}^{N_R}\sum_{v=1}^{\tau_n}\sum_{u=1}^{\tau_m}\delta^Z_{r_{m_u}r_{n_v}i}\langle\, E_i^M\mathbf{M}_{n_v}(\mathbf{r}'),\ \mathbf{J}_{m_u}(\mathbf{r})\,\rangle \\ &= \sum_{i=1}^{N_R}\sum_{v=1}^{\tau_n}\sum_{u=1}^{\tau_m}\delta^Z_{r_{m_u}r_{n_v}i}T^{T_jT_m}_{m_un_v} \\ &= -\sum_{i=1}^{N_R}\sum_{v=1}^{\tau_{n'}}\sum_{u=1}^{\tau_m}\delta^Z_{r_{m_u}r'_{n_v}i}\langle\, H_i^J\mathbf{J}'_{n_v}(\mathbf{r}'),\ \mathbf{J}_{m_u}(\mathbf{r})\,\rangle \\ &= -\sum_{i=1}^{N_R}\sum_{v=1}^{\tau_{n'}}\sum_{u=1}^{\tau_m}\delta^Z_{r_{m_u}r'_{n_v}i}T^{T_mT_j}_{m_un'_v} = -T^{T_mT_j}_{mn'}, \\ &\quad m=1,\ldots,N_{T_j}\text{ and } n=N_{T_j}+1,\ldots,N_{T_j}+N_{T_m} \end{aligned} \tag{26}$$

$$\begin{aligned} T_{mn}^{T_mT_j} &= \sum_{i=1}^{N_R}\sum_{v=1}^{\tau_n}\sum_{u=1}^{\tau_m}\delta^Z_{r_{m_u}r_{n_v}i}\langle\, H_i^J\mathbf{J}_{n_v}(\mathbf{r}'),\ \mathbf{M}_{m_u}(\mathbf{r})\,\rangle \\ &= \sum_{i=1}^{N_R}\sum_{v=1}^{\tau_n}\sum_{u=1}^{\tau_m}\delta^Z_{r_{m_u}r_{n_v}i}T^{T_mT_j}_{m_un_v}, \\ &\quad m=N_{T_j}+1,\ldots,N_{T_j}+N_{T_m}\text{ and } n=1,\ldots,N_{T_j} \end{aligned} \tag{27}$$

$$\begin{aligned} Y_{mn}^{T_mT_m} &= \sum_{i=1}^{N_R}\sum_{v=1}^{\tau_n}\sum_{u=1}^{\tau_m}\delta^Z_{r_{m_u}r_{n_v}i}\langle\, H_i^M\mathbf{M}_{n_v}(\mathbf{r}'),\ \mathbf{M}_{m_u}(\mathbf{r})\,\rangle \\ &= \sum_{i=1}^{N_R}\sum_{v=1}^{\tau_n}\sum_{u=1}^{\tau_m}\sum_{i=1}^{N_R}\sum_{v=1}^{\tau_n}\sum_{u=1}^{\tau_m}\delta^Z_{r_{m_u}r_{n_v}i}Y^{T_mT_m}_{m_un_v} \\ &= \sum_{i=1}^{N_R}\sum_{v=1}^{\tau_{n'}}\sum_{u=1}^{\tau_{m'}}\delta^Z_{r'_{m_u}r'_{n_v}i}\frac{1}{\eta_i^2}\,\langle\, E_i^J\mathbf{J}_{n'_v}(\mathbf{r}'),\ \mathbf{J}_{m'_u}(\mathbf{r})\,\rangle \\ &= \sum_{i=1}^{N_R}\sum_{v=1}^{\tau_{n'}}\sum_{u=1}^{\tau_{m'}}\delta^Z_{r'_{m_u}r'_{n_v}i}\frac{1}{\eta_i^2}\,Z^{T_jT_j}_{m'_un'_v}, \\ &m=N_{T_j}+1,\ldots,N_{T_j}+N_{T_m}\text{ and } n=N_{T_j}+1,\ldots,N_{T_j}+N_{T_m} \end{aligned} \tag{28}$$

$$\begin{aligned} V_m^{T_m} &= -\sum_{i=1}^{N_R}\sum_{u=1}^{\tau_m}\delta^F_{r_{m_u}i}\,\langle\,\mathbf{H}_i^{inc},\ \mathbf{M}_{m_u}(\mathbf{r})\rangle, \\ &\quad m=N_{T_j}+1,\ldots,N_{T_j}+N_{T_m}, \end{aligned} \tag{29}$$

where

$$\begin{aligned} \eta_i &= \sqrt{\mu_i/\epsilon_i} \\ J_{n'_v} &= M_{n_v} \\ J_{m'_u} &= M_{m_u}, \end{aligned} \tag{30}$$

and E_i^J, E_i^M, H_i^J, and H_i^M are the eld operators de ned in (14) and (15), and $\mathbf{B}_{n_v}$ is denoted by $\mathbf{J}_{n_v}$ and $\mathbf{M}_{n_v}$ to signify the electric and magnetic currents, respectively. Notice that in (26) and (28) the duality property of the eld operators is used and that there is one and only one $\mathbf{J}_{n'_u}$ which is the same as $\mathbf{M}_{n_u}$ for a dielectric interface. The prime in the subscript of $\mathbf{J}_{n'_u}$ is due to the fact that the indices n and n' are for the

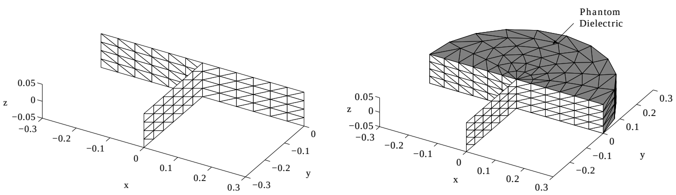

Fig. 3. Junction test case A — T-junctions with phantom dielectric.

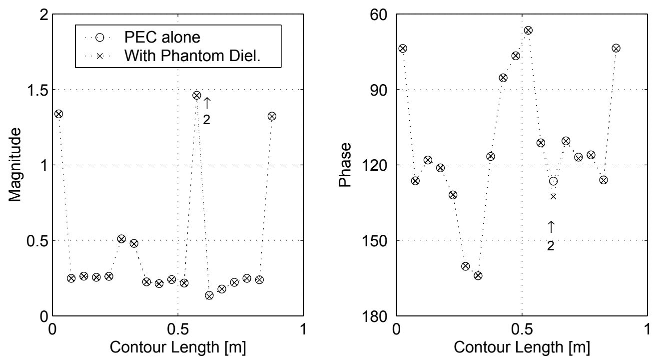

Fig. 4. z-directed current densities along the contours (○ - PEC alone, × - with phantom dielectric). The arrows denote the start of the second contour.

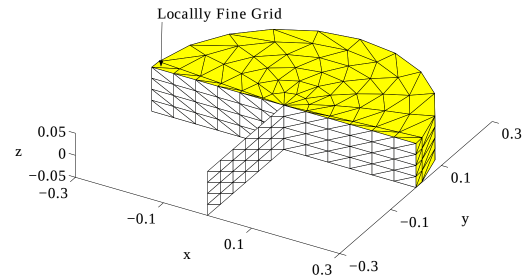

Fig. 5. Modeling with locally ne grids (Grid-3).

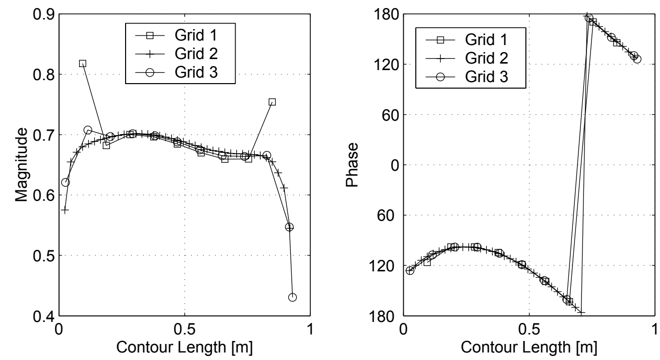

Fig. 6. ϕ-directed magnetic currents of T-junction with phantom dielectric along circumferential contour ($\phi=0°\rightarrow\phi=180°$, $z=0.0125$ m). Grid-1 and Grid-3 refer to grids shown in Figs. 3(b) and 5, respectively. Grid-2 is uniformly ne grid using 40 edges along the circumfernce.

generalized basis functions (n, $n^{'}=1, 2, \ldots, N$), and thus n and $n^{'}$ differ from each other for $\mathbf{J}_{n_u^{'}}$=$\mathbf{M}_{n_u}$.

Some subroutines of EMPACK [20] have been used for the integrations over the triangular domains which appear in (23) implicitly.

III. Numerical Results

A. Self Consistency Test — T-Junction

A T-shape junction of three 0.1-m wide and 0.3-m long PEC strips is taken as an example. For comparison, a semi-circular cylinder of phantom dielectric having 0.1-m height and 0.3-m radius is attached to the T-shape junction as shown in Fig. 3. The z-directed surface currents along the contour lines, $(-0.3,0,0)\rightarrow(0.3,0,0)$ and $(0,0,0)\rightarrow(0,-0.3,0)$, located at the center of each strip are computed for a plane wave excitation. The plane wave is expressed as $\mathbf{E}^{inc}=E_o\, e^{k_o\hat{k}^i\cdot\mathbf{r}}$, where $\hat{k}^i=-\hat{x}\cos\phi^i\sin\theta^i-\hat{y}\sin\phi^i\sin\theta^i-\hat{z}\cos\theta^i$, $E_o=E^i_\theta(\hat{x}\cos\theta^i\cos\phi^i+\hat{y}\cos\theta^i\sin\phi^i-\hat{z}\sin\theta^i)$, $\theta^i=\phi^i=45°$, $E^i_\theta=1$, $k_o=2\pi f\sqrt{\mu_o\epsilon_o}$, and $f=300$ MHz. The results in Fig. 4 show very good agreement as well as the expected current peaks at the ends of the strips.

The $\phi-$directed magnetic currents along a circumferential contour ($\phi=0°\rightarrow\phi=180°$, $z=0.0125$) are studied for three different grids. Grid-1 is shown in Fig. 3(b), and Grid-2 is a uniformly ne grid having 40 edges along the circumference. Grid-3 is similar to Grid-1, but it has locally ne grids near the conductor strips as shown in Fig. 5. As shown in Fig. 6, Grid-1 is not ne enough to result in the expected behavior of magnetic currents or electric elds near a conducting surface. At $\phi=0°$ and $\phi=180°$, where the conducting strips are located, the boundary conditions for the tangential electric eld dictates $E_z=0$ or $M_\phi=0$ at the conducting surface. The opposite trend of the numerical solution for M_ϕ near the conductor surface is due to the too coarse grid near the conductor, which cannot model the rapid eld variations properly. The locally ne grid, Grid-3, as well as the uniformly ne grid, Grid-2, result in the expected current distributions near the conducting surface. Similar behavior of the magnetic currents has been checked for a simple 0.1-m wide and 0.6-m long PEC strip without the center strip.

Fig. 7 shows the corresponding radar cross sections. It is worth noting that even Grid-1 results in very good agreement with the PEC-alone data in spite of the abnormal behavior of the magnetic currents described above.

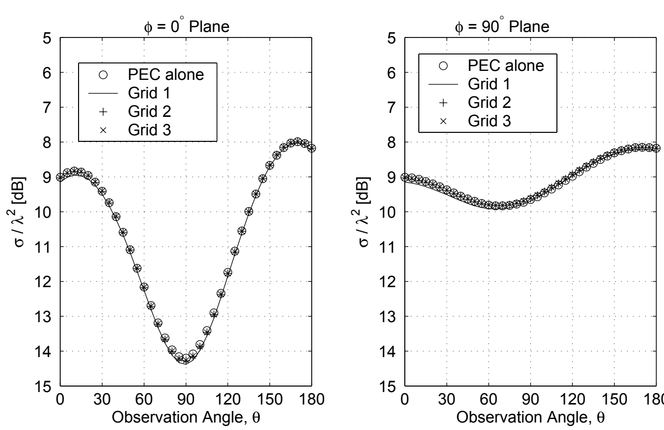

Fig. 7. RCS of T-junction with phantom dielectric.

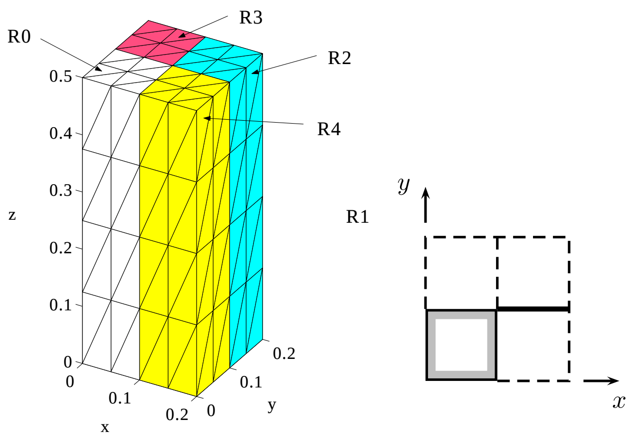

Fig. 8. Junction test case B — PEC block with three dielectric ones. Region R0 denotes conductor, and regions R2, R3, and R4 denote dielectric of ϵ_r=2, 3, and 4, respectively. The interface between R2 and R3 is dielectric, while that between R2 and R4 is PEC ($\mathcal{PF}2$). PF0-Model in Fig. 9 treats surface of PEC block as $\mathcal{PF}0$, while PF2-Model treats it as $\mathcal{PF}2$ with inside region being replaced by arbitrary dielectric. Units in m.

B. Self Consistency Test Using Two Different Models

In this section, a PEC square-bar with three dielectric ones attached to it as shown in Fig. 8 is considered. As shown in Fig. 9, the PEC bar can be modeled using either $\mathcal{PF}0$ or $\mathcal{PF}2$ surfaces. The surface of type $\mathcal{PF}0$ is modeled using one electric unknown, while $\mathcal{PF}2$ using two as discussed in section II. Moreover the process of assigning the basis functions and unknowns as described in the Appendix results in wildly different sets of unknowns as well as basis functions for the two models. The electric current distributions along twelve contours on the PEC bar and attached strip are plotted in Fig. 9 to show virtually the same results for the two different models. Each contour runs from $z = 0$ to $z = 0.5$, with (x, y) coordinates being (0.1, 0.0125), (0.1, 0.0375), (0.1, 0.0625), (0.1, 0.0875), (0.0875, 0.1), (0.0625, 0.1), (0.0375, 0.1), (0.0125, 0.1), (0.1125, 0.1), (0.1375, 0.1), (0.1625, 0.1), and (0.1875, 0.1) for contours 1 to 12, respectively. It should be noted that the results are obtained by using grid parameters for each block of `nex/ney/nez = 4/4/8` instead of `2/2/4` as suggested by the triangulation shown in Fig. 8 (`nex/ney/nez` are numbers of edges along x-, y-, and z-direction). The excitation parameters are $\theta^i = \phi^i = 45°$, $E_\theta^i = 1$, and $f = 300$ MHz.

C. Junction Tests Using FDTD

Extensive validation of the code for various types of junctions has been carried out. Here we present only sample results for the test case shown in Fig 10. It is a 0.1m × 0.1m × 0.5m dielectric bar of $\epsilon_r = 4$ with seven 0.1m × 0.1m PEC strips attached to it to result in $\mathcal{PF}1$-$\mathcal{DF}$-$\mathcal{PF}2$ and $\mathcal{PF}1$-$\mathcal{PF}2$-$\mathcal{PF}2$ junctions.

The top and bottom surfaces of the bar are dielectric. Fig. 11 shows good agreement between MoM and FDTD

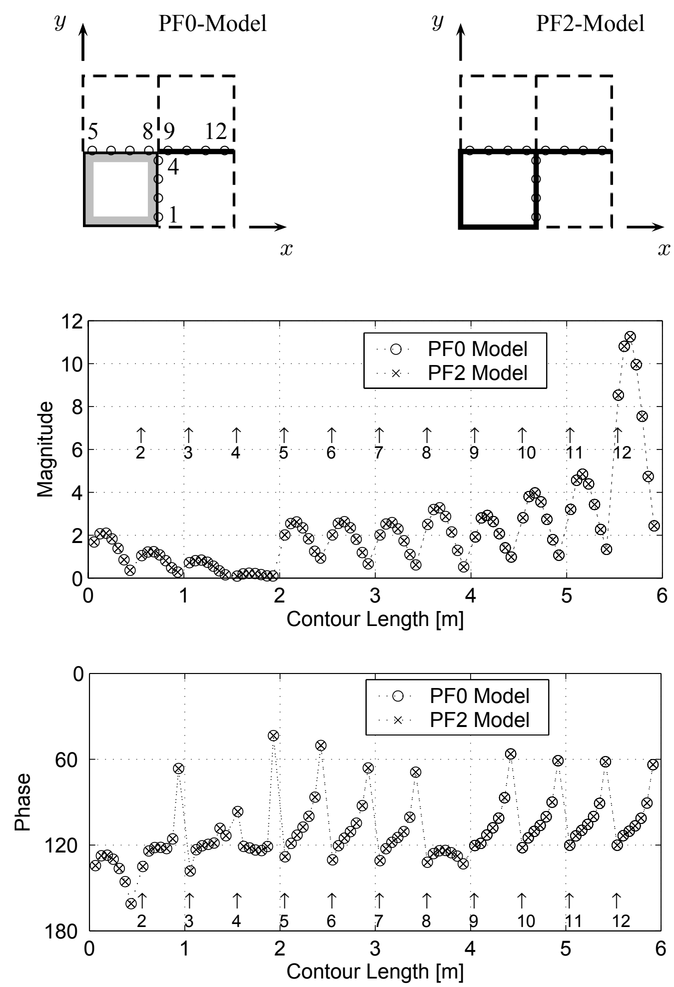

Fig. 9. Comparison of $z-$directed electric currents from two different models of PEC block shown in Fig. 8. Circles on geometry cross sections denote contour positions. Each contour runs from $z = 0$ to $z = 0.5$.

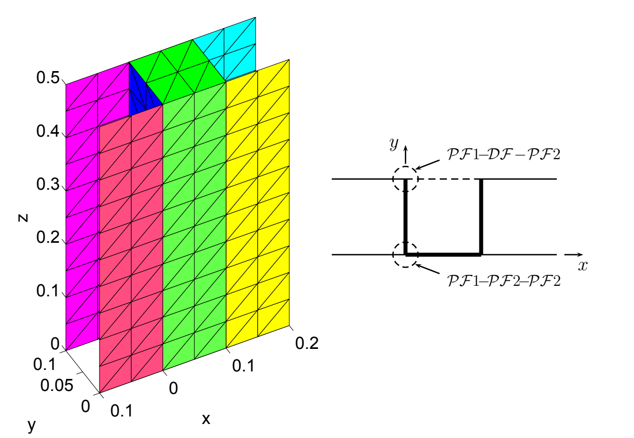

Fig. 10. Junction test case C — Dielectric bar with seven PEC strips. Units in m.

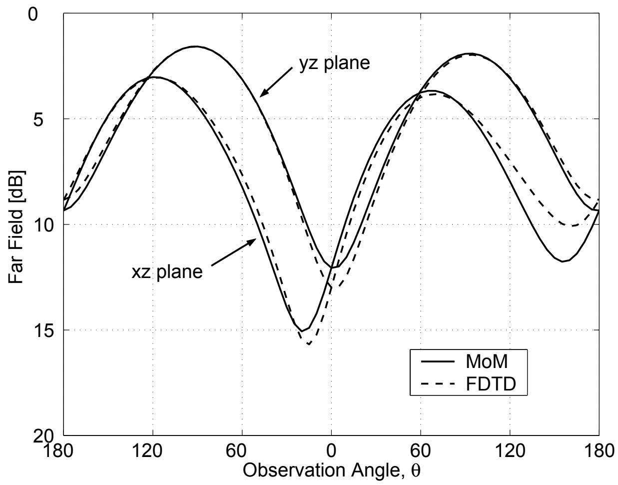

Fig. 11. Bistatic RCS for junction test case C shown in Fig. 10. $\theta^i = 45°$, $\phi^i = 30°$, $E^i_\theta = 1$, and $f = 300$ MHz.

(Finite Difference Time Domain) results except for around θ = 150° in xz-plane. The grid parameters are `nex/ney/nez = 3/3/10` for `ax/ay/az=0.1/0.1/0.5` (instead of `2/2/10` as suggested in Fig. 10), and the excitation parameters θ^i=45°, ϕ^i=30°, E^i_θ=1, and f=300 MHz. The FDTD parameters are: `dx = dy = dz =` 0.005 m, the second order Mur's RBC, 0.4-m distance from the scatterer boundary to the RBC, and a Gaussian pulse of with 0.4-ns width and 2-ns delay. The near- eld currents for the far- eld computation are sampled at surfaces ve cells away from the scatterer surfaces. The number of time steps used is 5000. However 2000 time steps should be enough.

D. Microstripline/Slot-Fed Rectangular DRA

A Rectangular DR Antenna (RDRA) fed by a microstripline through a narrow slot has been previously considered by Liu *et al.* [5]. The front and top views of such an RDRA are shown in Fig. 12. The geometry of the DR element and feed structure are taken from [5], where an in nite ground plane is assumed.

For the 3DIE code, the implementaion of the SIE/MoM formulation, a large nite ground plane is computationally expensive. It is even more expensive when the GP is backed by a substrate, in which case the GP PEC as well as the dielectric surface are modeled using two unknowns per edge. Thus, it is possible to reduce the number of unknowns signi cantly by truncating the substrate such that only a minimal portion of the substrate is used. The effect of the substrate truncation on the radiation patterns should be negligible as shown in Fig. 13. In Fig. 13, `x12y04f` and `x12y04` refer to the RDRAs with full and truncated substrates, respectively, while the numbers in them refer to the ground plane dimensions, $G_x = 12$ and $G_y = 4$, respectively, in cm.

We next verify that the 3DIE code computes the radiation patterns correctly and that the substrate truncation has no signi cant effects. Fig. 14 shows the MoM and FDTD computations of the radiation patterns of the smallest RDRA in the principal planes of $\phi = 0°/180°$ and $\phi = 90°/270°$. The

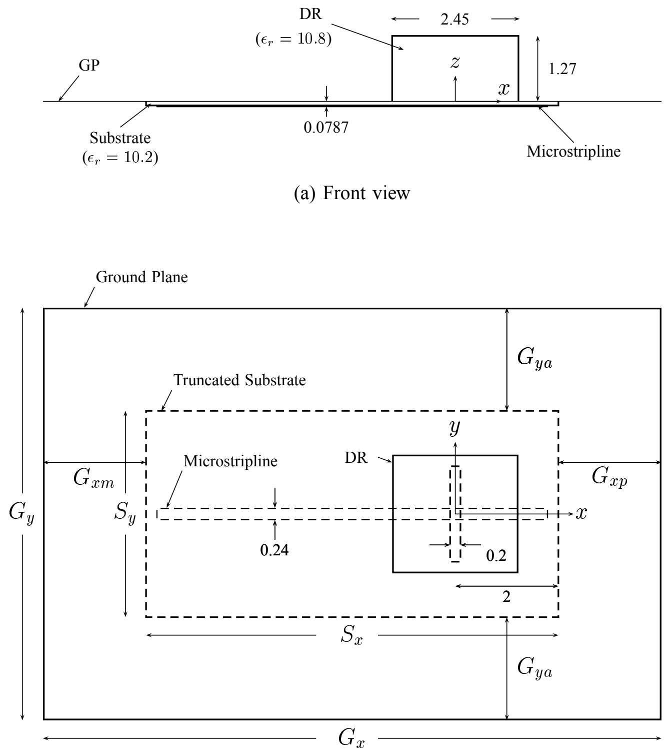

Fig. 12. RDRA with nite ground plane. DR dimensions are 2.45 × 2.5 × 1.27; slot length is 1.8; microstripline input and stub lengths are 5.8 and 1.8 from center of slot, respectively; S_x=8 and S_y=4, all in cm.

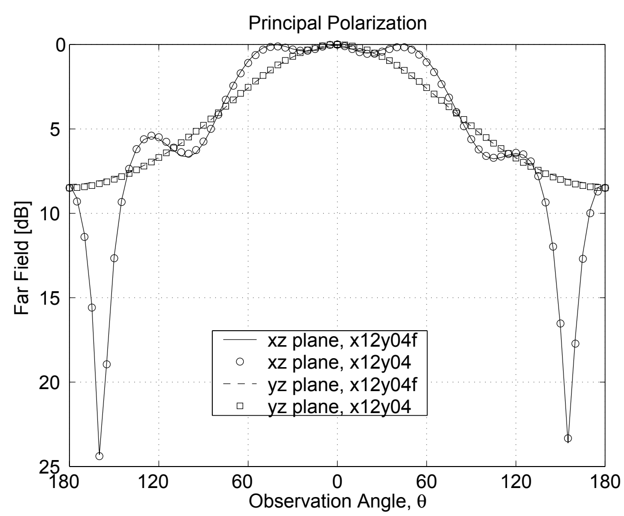

Fig. 13. Effect of substrate truncation of RDRA of Fig. 12 on radiation patterns with G_x=12, G_{xm}=0, G_{xp}=4, G_y=4, all in cm. RDRA `x12y04` has truncated substrate as shown in 12, while `x12y04f` has full substrate.

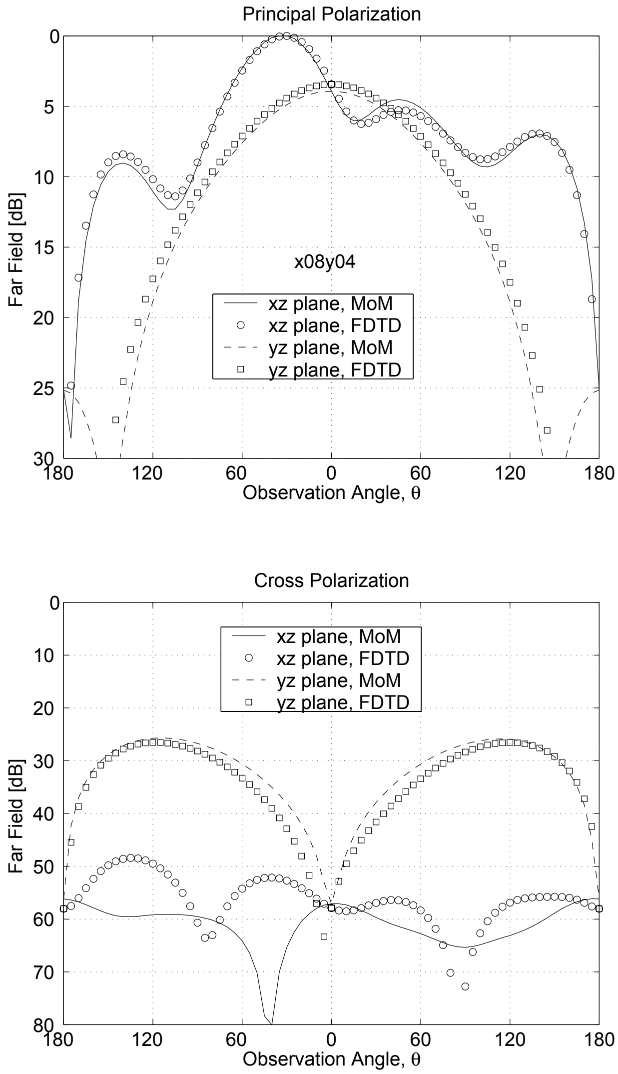

Fig. 14. Comparison of MoM and FDTD results for RDRA of Fig. 12 with $G_x = S_x = 8$ and $G_y = S_y = 4$, all in cm.

agreement between both methods is excellent for both the principal and cross polarization as shown in Fig. 14. It should be noted that the E-plane pattern (xz-plane principal polarization) shows high asymmetry. This is due to the asymmetry of the GP with respect to the DR element. The diffracted elds from the GP edges contribute differently to the elds radiated from the DR element due to the path differences in $\phi = 0°$ and $\phi = 180°$ planes. For RDRAs that have a symmetric GP, no such asymmetry has been observed in the radiation patterns. The cross polarization is shown to be low even for the minimal size of the GP. The effects of the nite ground plane size on the radiation patterns of the RDRA have been studied in [19].

IV. Conclusion

A systematic procedure for modeling of the general junctions of any combination of conducting and/or dielectric bodies in an SIE/MoM formulation has been presented. With the successful modeling of general junctions, it is possible to apply the E-PMCHWT formulation to a large class of problems including dielectric resonator antennas of complex con guration.

The procedure has been validated by modeling similar test structures in different manners and by comparison of results with FDTD solutions for a complex dielectric resonator antenna geometry.

V. Acknowledgment

This work was supported in part by The Army Research Of ce under grant No. DAAG55-98-0308.

References

[1] S. A. Long, M. W. McAllister, and L. C. Shen, "The resonant cylindrical dielectric cavity antenna," *IEEE Trans. Antennas Propagat.*, vol. AP-31, pp. 406–412, May 1983.

[2] T. E. Durham and C. G. Christodoulou, "Integral equation analysis of dielectric and conducting bodies of revolution in the presence of arbitrary surfaces," *IEEE Trans. Antennas Propagat.*, vol. AP-43, pp. 674–680, July 1995.

[3] G. P. Junker, A. A. Kishk, and A. W. Glisson, "Multiport network description and radiation characteristics of coupled dielectric resonator antennas," *IEEE Trans. Antennas Propagat.*, vol. AP-46, pp. 425–433, Mar. 1998.

[4] J. Y. Chen, A. A. Kishk, and A. W. Glisson, "Application of a new mpie formulation to the analysis of a dielectric resonator embedded in a multilayered medium coupled to a microstrip circuit," *IEEE Trans. Microwave Theory Tech.*, vol. MTT-49, pp. 263–279, Feb. 2001.

[5] Z. Liu, W. C. Chew, and E. Michielssen, "Numerical modeling of dielectric resonator antennas in a complex environment using the method of moments," *IEEE Trans. Antennas Propagat.*, vol. AP-50, pp. 79–82, Jan. 2002.

[6] S. U. Hwu and D. R. Wilton, "Electromagnetic scattering and radiation by arbitrary con gurations of conducting bodies and wires," Tech. Rep. TR 87-17, Applied Electromagnetics Laboratory, University of Houston, 1989.

[7] L. N. Medgyesi-Mitschang and J. M. Putnam, "Electromagnetic scattering from axially inhomogeneous bodies of revolution," *IEEE Trans. Antennas Propagat.*, vol. AP-32, pp. 797–806, Aug. 1984.

[8] J. M. Putnam and L. N. Medgyesi-Mitschang, "Combined eld integral equation formulation for inhomogeneous two- and three-dimensional bodies: The junction problem," *IEEE Trans. Antennas Propagat.*, vol. AP-39, pp. 667–672, May 1991.

[9] A. A. Kishk and L. Shafai, "Different formulations for numerical solution of single or multibodies of revolution with mixed boundary conditions," *IEEE Trans. Antennas Propagat.*, vol. AP-34, pp. 666–673, May 1986.

[10] J. M. Putnam and L. N. Medgyesi-Mitschang, "Generalized method of moments for three-dimensional penetrable scatterers," *J. Opt. Soc. Am. A.*, vol. 11, pp. 1384–1398, Apr. 1994.

[11] B. M. Kolundzija, "Electromagnetic modeling of composite metallic and dielectric structures," *IEEE Trans. Microwave Theory Tech.*, vol. MTT-47, pp. 1021–1032, July 1999.

[12] B. M. Kolundzija and R. D. Djordjevic, *Electromagnetic modeling of composite metallic and dielectric structures*. Artech House Inc., 2002.

[13] J. Poggio and E. K. Miller, *Integral equation solutions for three-dimensional scattering problems*. in *Computer Techniques for Electromagnetics*, R. Mitra, (ed.), Oxford, U.K.: Pergamon, 1973.

[14] Y. Chang and R. F. Harrington, "A surface formulation for characteristic modes of material bodies," *IEEE Trans. Antennas Propagat.*, vol. AP-25, pp. 789–795, Nov. 1977.

[15] T. K. Wu and L. L. Tsai, "Scattering from arbitrarily-shaped lossy dielectric bodies of revolution," *IEEE Trans. Antennas Propagat.*, vol. AP-, pp. 406–412, May 1983.

[16] M. Carr, E. Topsakal, and J. L. Volakis, "A procedure for modeling material junctions in 3-D surface integral equation approaches," *IEEE Trans. Antennas Propagat.*, vol. AP-52, pp. 1374–1379, May 2004.

[17] R. F. Harrington, *Time Harmonic Electromagnetic Fields*. McGraw-Hill, 1963.

[18] S. M. Rao, D. R. Wilton, and A. Glisson, "Electromagnetic scattering by surfaces of arbitrary shape," *IEEE Trans. Antennas Propagat.*, vol. AP-30, pp. 409–418, May 1982.

[19] J. Shin, *Modeling of arbitrary composite objects with applications to dielectric resonator antennas*. PhD thesis, University of Mississippi, 2001.

[20] S. V. Yesantharao, "EMPACK — A software toolbox of potential integrals for computational electromagnetics," Master's thesis, University of Houston, 1989.

APPENDIX

MODELING OF GENERAL SURFACE JUNCTIONS

For surface junctions, there may be infinitely many possible configurations regarding the number, order of connection, and types of the connected faces. Here, we develop a systematic procedure to model general junctions of arbitrary configuration.

A. Rules for Assigning Basis Functions and Unknowns

A single basis function is defined over a pair of any two adjacent triangular faces. Each basis function is associated with the region into which it radiates and its type may be either electric or magnetic. When at least one face of type $\mathcal{DF}$ is involved in the junction, several different basis functions may be related to the same unknown number, so we refer to this as a multi-domain basis function.

The types and numbers of the unknowns and basis functions of a junction, as well as the fashion in which they are assigned, are mainly determined by the boundary conditions of the fields on the connected faces. The field boundary condition on a PEC is that $E_{\tan} = 0$. Also the tangential magnetic field is discontinuous. The boundary conditions for a dielectric face are that the tangential electric and magnetic fields are continuous across the interface. From the $E_{\tan}=0$ condition, it follows that there is no magnetic current for a junction which has at least one PEC face. The continuity of fields across a dielectric face leads to the multiplicity of an unknown coefficient given by (8). For a $\mathcal{PF}2$ face, the discontinuous magnetic field results in two unknowns on each side of the face, while the total effect of the field on the two sides is represented by a single unknown on the face for a $\mathcal{PF}1$ face.

When all the connected faces are $\mathcal{PF}$ in the same region, the KCL (Kirchhoff's Current Law), which states that the sum of currents flowing into the junction edge from connected face is zero, is applied. In such a case, The numbers of basis functions and unknowns are $N_{tf}-1$ where N_{tf} is the number of the connected faces.

In the following sections, the above rules are used to derive the numbers of basis functions and unknown coefficients and to set up a systematic procedure for assigning basis functions and unknown coefficients.

B. Numbers of Basis Functions and Unknowns

For each edge, we have certain numbers of basis functions and unknowns related to it, which are determined by applying the rules of the previous section at the junction. For the purpose of convenience, general surface junctions are classified into three cases —

(i) All faces are $\mathcal{PF}1$
(ii) All faces are $\mathcal{DF}$
(iii) General cases excluding cases 1 and 2.

Then the numbers of basis functions n_b and unknowns n_u related to a junction edge can be expressed as follows

$$n_b = \begin{cases} n_{tf}-1, & n_{tf}=n_{pf1} \\ 2\,n_{tf}, & n_{tf}=n_{df} \\ n_{tf}-n_{pf0}/2, & \text{otherwise} \end{cases} \quad \text{(A-1)}$$

$$n_u = \begin{cases} n_{uj}=n_{tf}-1, & n_{tf}=n_{pf1} \\ n_{uj}+n_{um}=1+1=2, & n_{tf}=n_{df} \\ n_{tf}-n_{pf0}/2-n_{df}, & \text{otherwise} \end{cases} \quad \text{(A-2)}$$

where

n_b = number of basis functions related to a junction
n_u = number of unknowns related to a junction $= n_{uj}+n_{um}$
n_{uj} = number of electric unknowns
n_{um} = number of magnetic unknowns
n_{tf} = total number of faces connected to a junction $= n_{pf}+n_{df}$
n_{pf} = number of $\mathcal{PF} = n_{pf0}+n_{pf1}+n_{pf2}$
n_{pf0} = number of $\mathcal{PF}0$
n_{pf1} = number of $\mathcal{PF}1$
n_{pf2} = number of $\mathcal{PF}2$
n_{df} = number of $\mathcal{DF}$

Having the numbers of the basis functions and the unknowns for each edge, the corresponding total numbers are given as

$$N_b = \sum_{N_{edg}} n_b \quad \text{(A-3)}$$

$$N_u = N_{uj}+N_{um} = \sum_{N_{edg}} n_{uj} + \sum_{N_{edg}} n_{um} = \sum_{N_{edg}} n_u = N, \quad \text{(A-4)}$$

respectively, where N_{edg} is the number of edges in the problem.

C. Setting up Basis Functions and Unknowns

There are a number of legitimate ways to assign the basis functions and unknowns for a surface junction consisting of n_{tf} faces. Here, we describe a specific way which is chosen to facilitate convenient and systematic implementation of the code.

From the definition of the multi-domain RWG basis functions of (5)–(7), it is necessary to specify its type (electric or magnetic), positive/negative domains (from-face and to-face, i.e. the assumed positive current direction), and region for a basis function. While the determination of the type and region

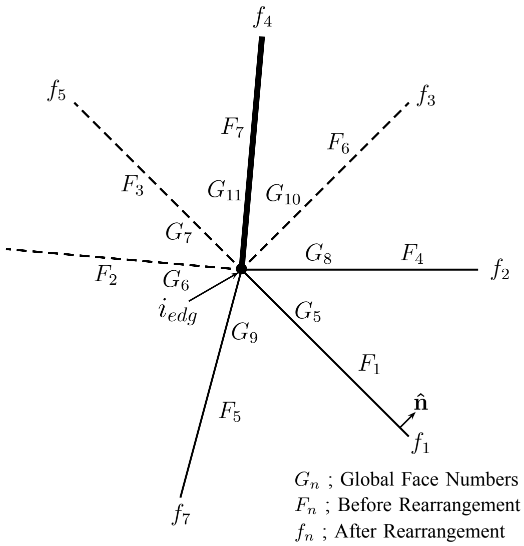

Fig. A-1. Rearrangement of local face numbers.

of the basis functions are relatively simple once their from-face and to-face are chosen, it is not a simple task to assign the from-face and to-face straightforwardly.

Initially the face numbers connected to a junction edge are listed in the order of increasing global face numbers. The resultant local face numbers may be spatially distributed without any order as shown in Fig. A-1. For a systematic junction modeling, it is necessary to rearrange them in an orderly manner. To this end, the rst face or the one with the lowest global number is chosen as the reference, from which the angles to others are measured. The direction of the increasing angle is determined by the surface normal of the reference face. Then consecutive local face numbers $(1,\ldots,n_{tf})$ are assigned to each face as shown in Fig. A-1. For the example shown the direction of increasing angle happened to be CCW (counter-clockwise) because of the surface normal $\hat{\mathbf{n}}$. When both PEC and dielectric faces are connected to an edge, the reference face must be a $\mathcal{PF}$. Thus if the lowest numbered face is a $\mathcal{DF}$, then the original local numbering is shifted until the reference becomes a $\mathcal{PF}$. Once the local face numbers are arranged in this way, we can determine the from-face, to-face, region number, type, and its unknown number straightforwardly. The from-face and to-face of the rst basis $(i_b = 1)$ are assumed to be the rst and second faces, respectively. Considering the rules of the section A at the junction and the resultant numbers of basis functions and unknowns of (A-1) and (A-2), the from-face and to-face of other basis functions $(i_b = 2, 3, \ldots, n_b)$ are determined as follows

(i) For $n_{tf} = n_{pf1}$ case (Fig. A-2(a)),

$$n_b = n_{tf} - 1 \tag{A-5}$$
$$ff = i_b \tag{A-6}$$
$$tf = i_b + 1 \tag{A-7}$$

(ii) For $n_{tf} = n_{df}$ case (Fig. A-2(b)),

$$n_b = 2\,n_{tf} \tag{A-8}$$
$$ff = \begin{cases} i_b, & i_b \le n_b/2 \quad (t_b = 1) \\ i_b + n_b/2, & i_b > n_b/2 \quad (t_b = 2) \end{cases} \tag{A-9}$$
$$tf = \begin{cases} i_b + 1, & i_b < n_b/2 \\ i_b + n_b/2 + 1, & n_b/2 < i_b < n_b \\ 1, & i_b = n_b/2 \quad \text{or} \quad i_b = n_b \end{cases} \tag{A-10}$$

(iii) For all other general cases (Fig. A-2(c)),

$$n_b = n_{tf} - n_{pf0}/2 \tag{A-11}$$
$$ff = \begin{cases} tf_p + 1, & tf_p \text{ is } \mathcal{PF}0 \\ tf_p, & \text{otherwise} \end{cases} \tag{A-12}$$
$$tf = \begin{cases} 1, & i_b = n_b \text{ and the last face is not } \mathcal{PF}0 \\ ff + 1, & \text{otherwise} \end{cases} \tag{A-13}$$

where

i_b = $2, 3, \ldots, n_b$ = consecutive indices for basis functions related to an edge
ff = local face number of the from-face of the i_b^{th} basis function $(1,\ldots,n_{tf})$
tf = local face number of the to-face of the i_b^{th} basis function $(1,\ldots,n_{tf})$
ff_p = ff of the $(i_b - 1)^{th}$ basis function
tf_p = tf of the $(i_b - 1)^{th}$ basis function
n_b = number of the basis functions related to an edge as given in (A-1)
t_b = type of basis function = $\begin{cases} 1, & \text{for electric} \\ 2, & \text{for magnetic.} \end{cases}$

The assignment of unknown numbers is self-explanatory in Fig. A-2(a) and (b) for cases (i) and (ii), respectively. For the general case of (iii), a new unknown number is assigned consecutively to each basis function unless the from-face is a dielectric face. When the from-face is a dielectric face, the previous unknown number is used again (see J_{3_2}, J_{3_3}, and J_{4_2} in Fig. A-2(c)). Thus, the multiplicity of an unknown is one if the related basis function does not have dielectric face for its domain. In general, τ_n, the multiplicity of an unknown number is given by

$$\tau_n = \begin{cases} n_{dfn}, & n_{dfn} = n_{tf} \\ n_{dfn} + 1, & \text{otherwise} \end{cases} \tag{A-14}$$

where

n_{tf} = total number of faces connected to the junction for I_n
n_{dfn} = number of dielectric faces related to I_n

Both J_1 and M_1 in Fig. A-2(b) have a multiplicity of four, while the unknowns J_5 and J_6 in Fig. A-2(c) have

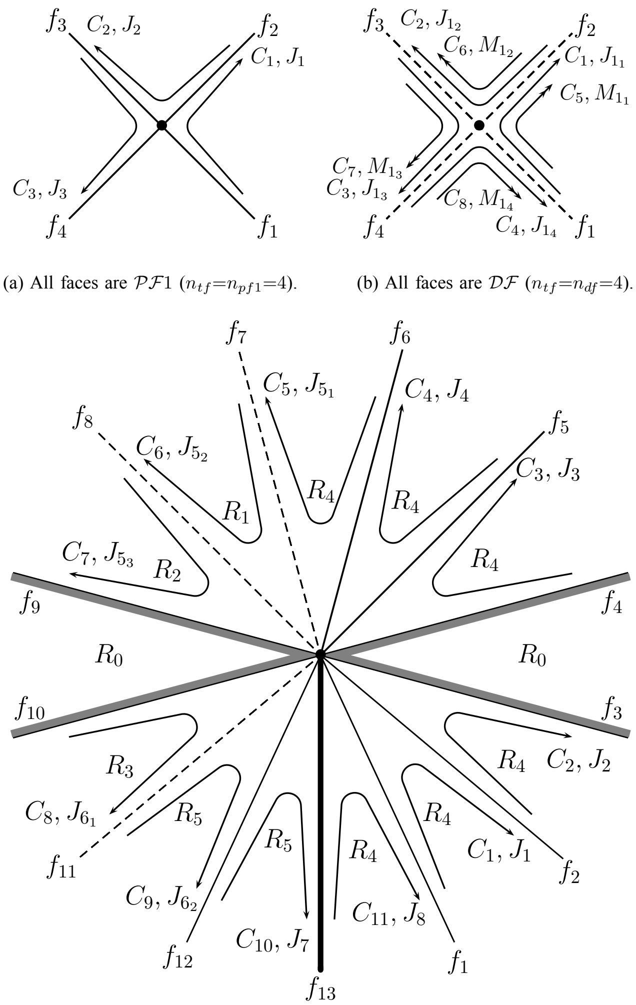

(a) All faces are $\mathcal{PF}1$ (n_{tf}=n_{pf1}=4). (b) All faces are $\mathcal{DF}$ (n_{tf}=n_{df}=4).

$$n_b = 13 - \tfrac{4}{2} = 11$$
$$n_u = 13 - \tfrac{4}{2} - 3 = 8$$

(c) A general case (n_{tf}=13, n_{pf0}=4, n_{pf1}=5, n_{pf2}=1, n_{df}=3).

Fig. A-2. Modeling of general surface junctions. (C_i, i=1, 2, 3, ..., is an entry-counting index.)

multiplicities of three and two, respectively. Notice that setting up the unknowns and basis functions of a given junction would be wildly different if the global edge or face numbers were set up differently.

After assigning the unknowns and the basis functions for all edges, it is possible to rearrange the order of the unknowns such that all electrical ones come before any magnetic ones so that the relationships in (5) hold.

Joon Shin received the B.E. and M.E. degrees in electrical engineering from the KyungPook National University, Korea, in 1981 and 1983, respectively. He earned the M.S. and Ph.D. degrees in electrical engineering from the University of Massachusetts at Amherst in 1996 and the University of Mississippi in 2001, respectively. He was employed at the Electromagnetics Laboratory of the Korea Research Institute of Standards and Science from 1982 to 1991 working on RF and microwave measurements. After working as a photonics design engineer at a private company, Anadigics Inc., NJ, for six months in 2001, he worked at the Electromagnetics Research Branch of the NASA Langley Research Center, Hampton, VA, as a National Research Council Research Associate in 2003. His current research interests are the development and application of numerical techniques (MoM, FDTD, and FEM) for treating electromagnetic problems.

Allen W. Glisson received the B.S., M.S., and Ph.D. degrees in electrical engineering from the University of Mississippi, in 1973, 1975, and 1978, respectively. In 1978, he joined the faculty of the University of Mississippi, where he is currently a Professor and Chair of the Department of Electrical Engineering. He was selected as the Outstanding Engineering Faculty Member in 1986, 1996, and 2004. His current research interests include the development and application of numerical techniques for treating electromagnetic radiation and scattering problems, and modeling of dielectric resonators and dielectric resonator antennas.

Dr. Glisson is a Fellow of the IEEE, a member of Commission B of the International Union of Radio Science, and a member of the Applied Computational Electromagnetics Society. Since 1984, he has served as the Associate Editor for Book Reviews and Abstracts for the IEEE Antennas and Propagation Society Magazine and he currently serves on the Board of Directors of the Applied Computational Electromagnetics Society. He has served as a member of the IEEE Antennas and Propagation Society Administrative Committee, as the secretary of Commission B of the U.S. National Committee of URSI, as an Associate Editor for Radio Science, as Co-Editor-in-Chief of the Applied Computational Electromagnetics Society Journal, and as Editor-in-Chief of the IEEE Transactions on Antennas and Propagation.

Ahmed A. Kishk received the BS degree in Electronic and Communication Engineering from Cairo University, Cairo, Egypt, in 1977, and in Applied Mathematics from Ain-Shams University, Cairo, Egypt, in 1980. In 1981 he joined the Department of Electrical Engineering, University of Manitoba, Winnipeg, Canada, where he obtained his M.Eng and PhD degrees in 1983 and 1986, respectively.

From 1977 to 1981, he was a research assistant and an instructor at the Faculty of Engineering, Cairo University. From 1981 to 1985, he was a research assistant at the Department of Electrical Engineering, University of Manitoba. From December 1985 to August 1986, he was a research associate fellow at the same department. In 1986, he joined the Department of Electrical Engineering, University of Mississippi, as an Assistant Professor. He was on sabbatical leave at Chalmers University of Technology during the 1994-1995 academic year. He is now a Professor at the University of Mississippi (since 1995). He was an Associate Editor of Antennas & Propagation Magazine from 1990 to 1993. He is now an Editor of Antennas & Propagation Magazine. He was a Co-editor of the special issue on Advances in the Application of the Method of Moments to Electromagnetic Scattering Problems in the ACES Journal. He was also an editor of the ACES Journal during 1997. He was an Editor-in-Chief of the ACES Journal from 1998 to 2001. He was the chair of Physics and Engineering division of the Mississippi Academy of Science (2001-2002).

His research interest includes the areas of design of millimeter frequency antennas, feeds for parabolic re ectors, dielectric resonator antennas, microstrip antennas, soft and hard surfaces, phased array antennas, and computer aided design for antennas. He has published over 120 refereed Journal articles and book chapters. He is a coauthor of the Microwave Horns and Feeds book (London, UK, IEE, 1994; New York: IEEE, 1994) and a coauthor of chapter 2 on Handbook of Microstrip Antennas (Peter Peregrinus Limited, United Kingdom, Ed. J. R. James and P. S. Hall, Ch. 2, 1989). Dr. Kishk received the 1995 outstanding paper award for a paper published in the Applied Computational Electromagnetic Society Journal. He received the 1997 Outstanding Engineering Educator Award from Memphis section of the IEEE. He received the Outstanding Engineering Faculty Member of the 1998. He received the Award of Distinguished Technical Communication for the entry of IEEE Antennas and Propagation Magazine, 2001. He received the 2001 Faculty research award for outstanding performance in research. He also received The Valued Contribution Award for outstanding Invited Presentation, "EM Modeling of Surfaces with STOP or GO Characteristics Arti cial Magnetic Conductors and Soft and Hard Surfaces" from the Applied Computational Electromagnetic Society. He received the Microwave Theory and Techniques Society Microwave Prize 2004. Dr. Kishk is a Fellow member of IEEE (Antennas and Propagation Society and Microwave Theory and Techniques), a member of Sigma Xi society, a member of the U.S. National Committee of International Union of Radio Science (URSI) Commission B, a member of the Applied Computational Electromagnetics Society, a member of the Electromagnetic Academy, and a member of Phi Kappa Phi Society.